4-Hydroxyphenylacetate Decarboxylases: Properties of a Novel Subclass of Glycyl Radical Enzyme Systems†

Lihua Yu, Martin Blaser, Paula I. Andrei, Antonio J. Pierik, and Thorsten Selmer*

Laboratorium für Mikrobiologie, Philipps-Universität, Karl-von-Frisch-Strasse 8, D-35032 Marburg, Germany

Received April 28, 2006; Revised Manuscript Received June 12, 2006

ABSTRACT: The 4-hydroxyphenylacetate decarboxylases from *Clostridium difficile* and *Clostridium scatologenes*, which catalyze the formation of *p*-cresol, form a distinct group of glycyl radical enzymes (GREs). Cresol formation provides metabolic toxicity, which allows an active suppression of other microbes and may provide growth advantages for the producers in highly competitive environments. The GRE decarboxylases are characterized by a small subunit, which is not similar to any protein of known function in the databases, and provides unique properties that have not been observed in other GREs. Both decarboxylases are functional hetero-octamers ($\beta_4\gamma_4$), which contain iron−sulfur centers in addition to the glycyl radical prosthetic group. The small subunit is responsible for metal binding and is also involved in the regulation of the enzymes' oligomeric state and activity, which are triggered by reversible serine phosphorylation of the glycyl radical subunits. Biochemical data suggest that the iron−sulfur centers of the decarboxylases could be involved in the radical dissipation of previously activated enzymes in the absence of substrate. The cognate activating enzymes differ from their Pfl and Nrd counterparts in that up to two iron−sulfur centers, in addition to the characteristic SAM cluster, were found. Biochemical data suggested that these [4Fe−4S] centers are involved in the electron transfer to the SAM cluster but do not directly participate in the reductive cleavage of SAM. These data imply a tight regulation of *p*-cresol formation, which is necessary in order to avoid detrimental effects of the toxic product on the producers.

Glycyl radical enzymes (GREs)[1] are important and versatile biocatalysts, which enable anaerobes to catalyze chemically difficult reactions under strictly anoxic conditions (*1*−*4*). These enzymes are generally synthesized as large (about 100 kDa) precursor polypeptides and require post-translational activation by dedicated iron−sulfur proteins for catalytic activity. The GRE activating enzymes (AEs) are members of the *S*-adenosylmethionine (SAM) radical enzyme superfamily (*5*) and catalyze the reductive cleavage of SAM to yield methionine and a 5′-deoxyadenosyl radical (*6*−*12*). The latter is used to abstract the *pro-S*-hydrogen atom from the α-carbon of a specific glycyl residue, that is located close to the C-terminus of the enzyme, and forms part of a characteristic and strictly conserved amino acid fingerprint motif (*13*, *14*) in all GREs. The protein-bound radical is essential for catalytic activity and causes extreme sensitivity of the GREs toward molecular oxygen (*14*). In the absence of oxygen, however, the radical, which is stabilized by the captodative effect of the neighboring peptide bonds, can persist in the protein for hours. The crystal structures of class III ribonucleotide reductase (Nrd, (*15*)), pyruvate formate-lyase (Pfl, (*16*, *17*)), and of the coenzyme B_{12}-independent glycerol dehydratase (Gdh, (*18*)) revealed that GRE precursor proteins lacking the essential radical consist of 10-stranded β-barrel cores surrounded by α-helices in each monomer. Two loops, protruding into the center of the β-barrel, contain either the conserved glycine of the C-terminal domain that is converted to the radical, or a conserved cysteine located in the middle of the amino acid sequence. During catalysis, the enzyme-bound radical moves from the glycyl residue to this active-center cysteine, forming a thiyl radical that mediates catalysis.

GREs generally occur as homodimeric proteins, which carry only one glycyl radical per native dimer (*9*, *13*, *14*). However, two of the recently identified GREs differ from this general theme in that these enzymes contain additional small subunits (*4*). Benzylsuccinate synthase (Bss, EC 4.1.99.11) from *Thauera aromatica* was the first hetero-oligomeric GRE described (*19*). This enzyme initiates the anaerobic degradation of toluene in nitrate-reducing bacteria, a radical-mediated addition of the methyl group of toluene to the double bond of fumarate (*19*, *20*). Bss is a hetero-hexamer ($\alpha_2\beta_2\gamma_2$) of three different subunits with molecular masses of 98, 8.5, and 6.5 kDa. Only its large subunit is similar to other glycyl radical enzymes, whereas the two small subunits are unique to Bss.

4-Hydroxyphenylacetate (HPA) decarboxylase (Hpd, EC 4.1.1.82) catalyzes the formation of *p*-cresol (4-methylphe-

† This study was supported by the Deutsche Forschungsgemeinschaft (Grants SE/1-3).

* Correponding author. Thorsten Selmer, Laboratorium für Mikrobiologie, Karl-von-Frisch-Str. 8, D-35032 Marburg, Germany. Tel., +49-6421-2823478; fax, +49-6421-2828979; e-mail, selmer@staff.uni-marburg.de.

[1] Abbreviations: AE, activating enzyme; Bss, benzylsuccinate synthase; Csd, 4-hydroxyphenylacetate decarboxylase from *Clostridium scatologenes*; DHPA, 3,4-dihydroxyphenylacetate; DTT, dithiothreitol; EPR, electron paramagnetic resonance; Gdh, vitamin B_{12}-independent glycerol dehydratase; GRE, glycyl radical enzyme; HPA, 4-hydroxyphenylacetate; Hpd, 4-hydroxyphenylacetate decarboxylase from *Clostridium difficile*; Nrd, class III ribonucleotide reductase; Pfl, pyruvate formate-lyase; SAM, *S*-adenosylmethionine; TFA, trifluoroacetic acid.

10.1021/bi060840b CCC: $33.50
Published on Web 07/08/2006

nol) by the human pathogenic bacterium *Clostridium difficile* (*21*, *22*). The genes encoding two subunits of the decarboxylase (*hpdB* and *hpdC*) and its cognate AE (*hpdA*) have been recently cloned and expressed in *Escherichia coli* (*23*). The two decarboxylase genes encode a novel member of the GRE family (902 amino acids), and a small subunit of 85 amino acids, which was originally overlooked and showed no similarity to other proteins in the databases (*24*). The coexpression of both decarboxylase genes was essential in order to obtain soluble protein in *E. coli* (*23*). The radical-free recombinant decarboxylase is a hetero-octamer ($\beta_4\gamma_4$) that could be activated by the recombinant AE in vitro. However, the endogenous enzyme from *C. difficile* was in the radical form a homodimer of large subunits (*24*). Its specific activity was 2 orders of magnitude lower than the recombinant enzyme after in vitro activation, and it has been suggested that loss of the small subunit causes inactivation during the purification of the endogenous enzyme (*23*).

The formation of *p*-cresol as end-product of tyrosine fermentation has been also reported for *Clostridium scatologenes* (*21*). This organism has been named according to its ability to form 3-methylindole (scatole). Scatole is formed by decarboxylation of indole-3-acetate, and the initial characterization of the reaction in cell-free extracts suggested that another GRE decarboxylase could be involved (*24*).

In this communication we report a comprehensive study of the HPA decarboxylase systems from *C. difficile* (Hpd) and *C. scatologenes* (Csd), which defines novel properties of a distinct subclass of GREs that clearly differs from previously studied systems.

MATERIALS AND METHODS

Materials. C. scatologenes 957^T was from DSMZ (Braunschweig, Germany). All chemicals used were purchased from Sigma-Aldrich (Deisenhofen, Germany), Lancaster (Mühlheim, Germany), or Merck (Darmstadt, Germany) and were of the highest quality available. Molecular biology tools were from Roche (Mannheim, Germany), MBI Fermentas (St. Leon-Rot, Germany), Amersham (Freiburg, Germany), Qiagen (Hilden, Germany), or Peqlab Biotechnology (Erlangen, Germany). Plasmid DNAs were from Stratagene (La Jolla, CA, pBluescript II SK$^+$), Invitrogen (Karlsruhe, Germany, pCR2.1), or IBA (Göttingen, Germany, pASK-IBA7). Custom sequencing of PCR-products or -vectors and primer syntheses were performed by MWG-Biotech (Ebersberg, Germany).

Methods. 1. Sequencing of the csd Locus from C. scatologenes. The unique genetic arrangement of the *hpd* locus in the genome of *C. difficile* suggested that a corresponding system(s) in *C. scatologenes* may exhibit a similar genetic arrangement. On the basis of this assumption, a degenerate forward primer corresponding to conserved glycyl radical motif and a reverse primer based on the SAM radical cluster motif of the AE gene were deduced. These primers amplified a 500 bp fragment from the genomic DNA of *C. scatologenes*, which was sequenced. In addition to the 3′-end of a GRE decarboxylase gene (*csdB*) and the 5′-end of its cognate AE gene (*csdA*), the fragment contained an ORF encoding a small subunit gene (*csdC*) located between these genes.

The entire *csd* locus of *C. scatologenes* was cloned and sequenced from restriction endonuclease-digested genomic DNA by a combination of PCR-based techniques. *XbaI* fragments were ligated into pBluescript II SK$^+$ in order to provide M13-derived primer binding sites on the distal sites of the target. The vector-ligated fragments were templates for PCR amplifications with insert-specific primers and M13-primers (Lig-PCR). Genomic *PstI*-fragments were used as templates in a TOPO Walker approach according to the manufacturer's instructions. *NdeI* or *HindIII* fragments were circularized in diluted solution and subsequently used as template with two target-derived, divergent primers in inverse PCRs. The PCR products thus obtained were gel-purified and either directly sequenced with the primers used for amplification or cloned into pCR2.1 prior to sequencing with vector-derived M13 primers.

The DNA sequence encoding the *csd* locus from *C. scatologenes* was deposited under accession number DQ227741 in the GenBank database at NCBI.

2. Generation of Expression Plasmids. To minimize PCR errors, a Hi-Fidelity DNA polymerase (Hi-Fidelity-PCR Enzyme mix, Abgene) was used for PCR amplification of the individual genes from genomic DNAs. The genes encoding both subunits of the decarboxylases were co-amplified and inserted together in expression vectors, while the AE genes were cloned individually. To facilitate purification of the recombinant proteins, the glycyl radical subunit genes and the AE genes were N-terminally fused to a Strep-Tag in pASK-IBA7. Primers containing mutagenic extensions generated *SacII* or *BamHI* sites, which allowed a directed cloning of the genes. The pASK-IBA7-derived plasmids were propagated in DH5α cells, and the DNA sequences of the inserts were determined on both strands.

3. Gene Expression and Protein Purification. Recombinant proteins were produced in Rosetta (DE3) pLysS cells kept under selection with carbenicillin (50 μg/mL) and chloramphenicol (34 μg/mL) during aerobic growth. Cells were grown at 28 °C (decarboxylases) or 22 °C (activating enzymes) and induced at $OD_{578\,nm}$ of 0.6−0.8. The cells were stressed by the addition of 2% [v/v] ethanol 30 min prior to induction with anhydrotetracylin (50 μg/L for AEs and 100 μg/L for decarboxylases) and harvested by centrifugation 3−4 h post induction. Cell pellets were stored frozen at −80 °C.

All purification steps and enzyme assays were performed in an anoxic glovebox with a N_2/H_2 (95%/5%) atmosphere. The cells (3−5 g) were suspended in anoxic buffer BC (100 mM Tris/HCl, 150 mM NaCl, 5 mM $(NH_4)_2SO_4$, 5 mM $MgCl_2$, and 5 mM DTT, pH 7.5) supplemented with 0.2 mM $Fe(NH_4)_2(SO_4)_2$, 5 mM cysteine, and 5 mM ATP for homogenization. The cell suspension was sonicated at 50 W for 2 × 5 min with a Branson sonifier (Branson Ultrasonics, Danbury, CT) under cooling with ice-H_2O. Cell debris were removed by centrifugation at 100 000*g* for 60 min at 18 °C. The clear supernatant was loaded onto 5 mL Streptactin-Macroprep columns, and the recombinant enzyme was eluted according to the manufacturer's instructions in buffer BC. The AEs were purified likewise in the same buffer plus 50 mM arginine and 50 mM glutamate at pH 8.

The resulting enzyme preparations were concentrated in Vivaspin concentrators (Vivascience, Hannover, Germany) with suitable cutoffs. Individual enzyme preparations were used immediately or stored at −80 °C. Protein concentrations were derived from the absorbance at 280 nm in 0.1%

trifluoroacetic acid (TFA), 4 M guanidinium hydrochloride, and calculated molar extinction coefficients.

4. Subunit Composition and Fe/S Content. Native molecular masses were determined as previously described (*23*, *24*). The subunit composition of the decarboxylases were determined by RP-HPLC on Aquapore-RP300_Bu columns (2.1 × 100 mm, Brownlee) operated in a 0.1% TFA-modified water/acetonitrile gradient. The integrated signals at 280 nm were corrected for different molar extinction coefficients to establish the molar ratio of large and small subunits.

UV/vis spectroscopy of the recombinant enzymes was carried out in rubber-stoppered quartz cuvettes with a Hewlett-Packard P 8453 diode array photometer. Non-heme iron was determined with ferene and acid-labile sulfide with *N*,*N*′-dimethyl-*p*-phenylene-diamine (*25*).

5. Enzyme Activity Assays. The enzyme activities were determined at molar ratios of decarboxylases to AEs of 1:4 in 100 mM Tris-HCl, pH 7.5, 40 mM NaCl, 5 mM $MgCl_2$, 5 mM $(NH_4)_2SO_4$, 5 mM cysteine, 25 mM substrate, and 5 mM DTT supplemented with either titanium(III) citrate (2.5 mM) and sodium sulfite (2 mM), or sodium dithionite (2 mM). The enzymes were prereduced for 30 min at 30 °C prior to addition of SAM (250 μM final concentration). At various time points, samples were withdrawn, the reaction stopped by perchloric acid precipitation, and analyzed for product formation by RP-HPLC (*24*). Preactivation experiments were carried out at 20-fold higher protein concentrations in buffers without substrate. Aliquots were taken at various time points and assayed for activity.

To obtain comparable results for the kinetic experiments, the enzymes were briefly (5 min) activated prior to activity measurements at various substrate concentrations. The specific activities were calculated from the product formation at time intervals of 2 min for total assay times of 18 min. These data were fitted to the Michaelis−Menten equation using the "Solver" facility provided by Excel 2000 in order to minimize V_{max} and K_m errors. Turnover numbers were calculated based on a molecular mass of 440 kDa with one glycyl radical site per hetero-octameric decarboxylase.

6. EPR Spectroscopy. X-band EPR spectra were obtained with a Bruker ESP-300E EPR spectrometer equipped with an ER-4116 dual mode cavity and an Oxford Instruments ESR-900 helium-flow cryostat and an ITC4 temperature controller.

EPR samples were prepared in assay buffer in fully oxygen-protected environments. Activity tests were performed for individual samples in order to correlate glycyl radical content with specific activity. Unless otherwise stated, glycyl radical measurements were carried out at 77 K, while iron−sulfur centers were measured at 10 K. Spin integration was carried out under nonsaturating conditions using 10 mM $CuSO_4$ in 2 M $NaClO_4$/10 mM HCl as standard.

7. Western Blots. C. difficile was cultivated in a defined minimal medium (*26*) with or without HPA. The cells were harvested under anoxic conditions, and cell-free extracts were prepared. These extracts were immediately subjected to SDS−PAGE and blotted onto Protean BA83 nitrocellulose membranes (Schleicher & Schuell, Dassel, Germany). The membranes were treated with blocking solution (Sigma). Serine phosphorylation was detected with monoclonal antibodies (Qiagen) according to the supplier's instructions. The membranes were then stripped with 50 mM sodium hydroxide and 1% (w/v) SDS and reanalyzed with HpdBC-specific rabbit antiserum, which was raised according to standard laboratory protocols. Signals were detected using horseradish peroxidase-coupled secondary antibodies together with luminol/*p*-hydroxycoumaric acid chemoluminescence on Fuji 100 NIF medical X-ray films.

Table 1: Physicochemical Properties of the Recombinant HPA Decarboxylases and Their Cognate AEs[a]

protein	native molecular mass [kDa]	oligomeric state	iron atoms per native molecule
Csd-AE	37	α	5-**8.5**-9
Hpd-AE	38	α	6-**7.2**-11
Csd	440	$\beta_4\gamma_4$	26-**31**-32
Hpd	445	$\beta_4\gamma_4$	28-**30**-32

[a] The iron content of various ($n > 5$) individual preparations (minimum-**average**-maximum) is given per native structure.

RESULTS

Earlier studies regarding the properties of HPA decarboxylases were hampered by the restriction to an individual system from *C. difficile* (Hpd) and by the fact that both the endogenous and the recombinant enzymes were unstable (*23*, *24*). To overcome these difficulties, HPA decarboxylase from *C. scatologenes* (Csd) was included in this study. This allowed comparative studies of the enzymes, which share 58% amino acid sequence identities between the glycyl radical subunits. The limited stability of recombinant enzymes was overcome by genetic fusion of the glycyl radical subunit and the AE genes to an N-terminal Strep-tag, which facilitated purification and yielded stable enzyme preparations. In contrast to the homodimeric GREs, pyruvate formate lyase (Pfl), anaerobic ribonucleotide reductase (Nrd), and coenzyme B_{12}-independent glycerol dehydratase (Gdh), HPA decarboxylases are hetero-oligomeric iron−sulfur proteins, composed of large glycyl radical subunits (∼100 kDa) and of unique small subunits (∼9.5 kDa). According to size-exclusion chromatography, recombinant Hpd and its homologue from *C. scatologenes* were hetero-octameric ($\beta_4\gamma_4$) proteins and contained 30−32 irons and 28−32 acid-labile sulfurs (Table 1). The oxygen-sensitive recombinant decarboxylase AEs were monomeric proteins with molecular masses of about 37 kDa and contained on average 8 irons and 8 acid-labile sulfurs per molecule. Thus, the metal content of decarboxylase AEs was significantly larger than the metal content of Pfl- or Nrd-AEs, exclusively containing the SAM cluster with 4 irons and 4 sulfurs. UV−visible spectroscopy revealed broad charge-transfer signals between 300 and 800 nm without fine structure, which partially bleached upon dithionite reduction. This suggests that only $[4Fe-4S]^{+1/+2}$ centers were contained. The molar extinction coefficients at 400 nm suggested presence of up to 4−6 clusters per hetero-octamer in Hpd (60−65 mM^{-1} cm^{-1}) and Csd (75−88 mM^{-1} cm^{-1}), and approximately 2 in the cognate monomeric AEs (13−36 mM^{-1} cm^{-1} for Hpd-AE and 24−28 mM^{-1} cm^{-1} for Csd-AE) (Figure 1).

The iron−sulfur clusters in the Hpd and Csd systems were studied by EPR spectroscopy. The as-purified AEs were almost EPR-silent, but upon sodium dithionite-reduction, axial $S = 1/2$ EPR signals with $g_x = 2.04$ and $g_{yz} = 1.94$ were observed below 30 K (Figure 2, traces A). Only

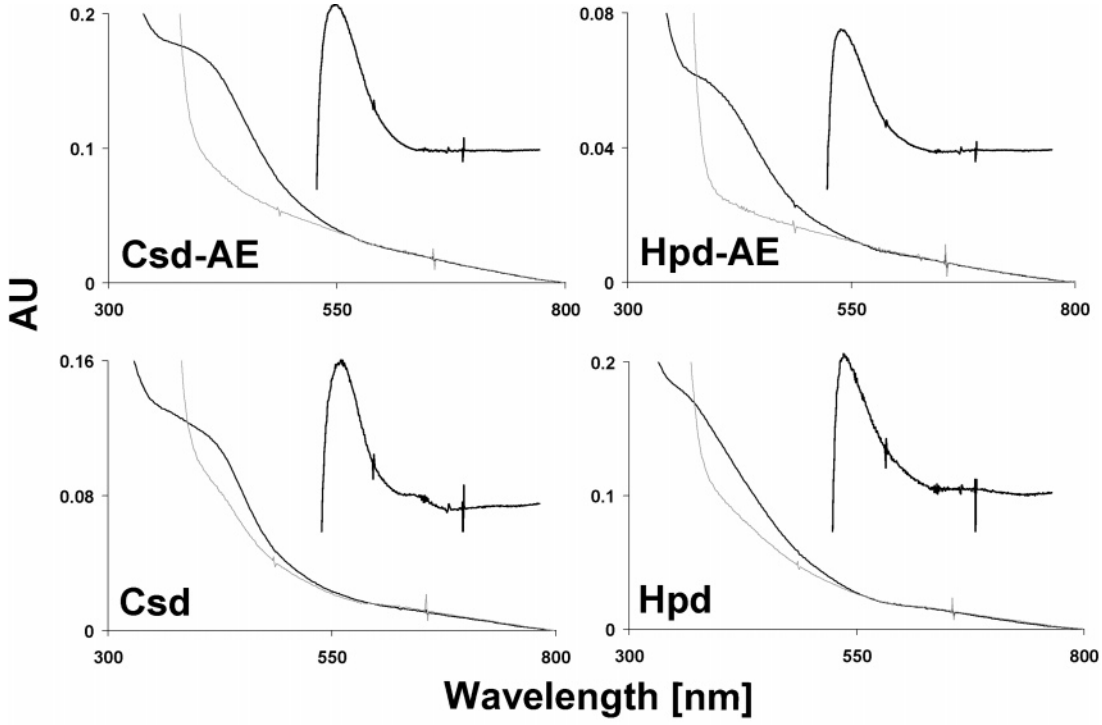

FIGURE 1: UV-visible spectra of the decarboxylases and their cognate AE. Freshly purified enzymes (2.5 μM Csd and Hpd, 5 μM HpdA, 10 μM CsdA) were measured in the respective anoxic purification buffer (black lines). Reduction with sodium dithionite (1mM) for 1 h at room temperature partially bleached the absorbance (gray lines). The insets show the difference spectra between the freshly purified and the dithionite-reduced samples.

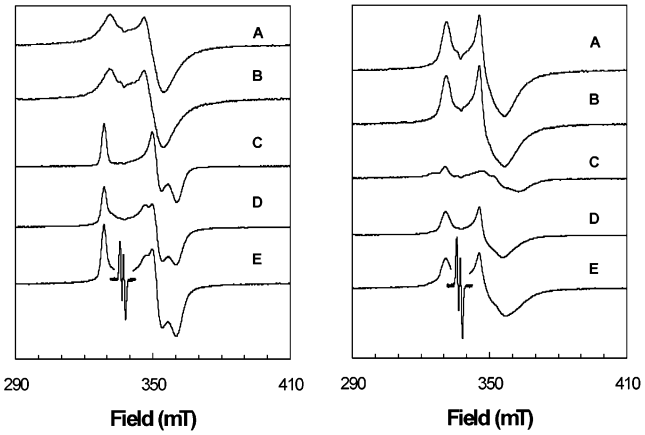

FIGURE 2: EPR spectra of metal centers in HPA decarboxylases and the cognate AEs from *C. difficile* (left) and *C. scatologenes* (right). The spectra were recorded at 10 K (microwave power, 0.8 mW; frequency, 9.460 GHz; modulation frequency, 100 kHz; amplitude, 1.25 mT). Amplitudes can be directly compared as no scaling was applied. The insets in traces E were collected at the nonsaturating settings of Figure 3. All samples were reduced with sodium dithionite (1 mM) for 30 min plus 5 min for samples containing SAM and frozen in liquid nitrogen. The protein concentrations were 5 mg/mL for the AEs and 4 mg/mL for the decarboxylases. (A) AE-reduced, (B) AE plus SAM (250 μM), (C) decarboxylases-reduced, (D) AE plus decarboxylase-reduced, (E) AE plus decarboxylase plus SAM (250 μM).

marginal changes in EPR signal intensities and signal shape were observed upon addition of SAM (Figure 2, traces B). The observed *g*-values and temperature dependence of the relaxational behavior are in agreement with the presence of [4Fe−4S] centers as suggested by UV/visible spectroscopy. Spin integration showed 0.2−0.3 reduced [4Fe−4S] centers, suggesting that only 7−15% of the total 2−3 iron−sulfur centers were reduced in the AEs. These values were significantly lower than expected from UV−visible measurements, suggesting that either partial damage of the metal centers upon freezing occurred or a significant portion of the reduced iron−sulfur centers were in spin 3/2 state.

EPR spectroscopy of the decarboxylases provided additional evidence for iron−sulfur centers in GREs (Figure 2, traces C). The dithionite-reduced Hpd showed an intense rhombic signal with *g*-values of 2.054, 1.921, and 1.87, which integrated to 2.9 spins/($\beta_4\gamma_4$). In Csd, a mixture of two rhombic species with $g_x = 2.074/2.044$, $g_y = 1.937/1.906$, and $g_z \sim 1.86$ was found, which integrated to 1.3 spins/($\beta_4\gamma_4$). These signals broadened out above 30 K, supporting the $[4Fe-4S]^{+1/+2}$ centers indicated by UV/visible spectroscopy. The coreduction of the decarboxylases with the cognate AEs yielded EPR spectra (Figure 2, traces D), which are readily explained by summation of spectra of the individual proteins. The addition of SAM (Figure 2, traces E) caused rapid formation of the glycyl radical prosthetic groups, but did not alter the redox state of the iron−sulfur clusters in the individual proteins.

The intense glycyl radical signal superimposes upon the iron−sulfur-derived spectral features at low temperatures but is the only detectable signal at >60 K (Figure 3). The glycyl radical signals of in vitro activated recombinant decarboxylases (Figure 3B,C) were similar to those reported previously for Pfl (*14*) and Nrd (*9*). They were almost indistinguishable from Bss (*27*) or endogenous decarboxylase from *C. difficile* (Figure 3A), that is, isotropic doublets with a *g*-value of 2.0034 and a hyperfine coupling of 1.45−1.5 mT to the remaining proton at the sp^2-hybridized glycyl radical. This proton rapidly exchanged with solvent D_2O (Figure 3D) in HPA decarboxylases. The maximum signal intensities ob-

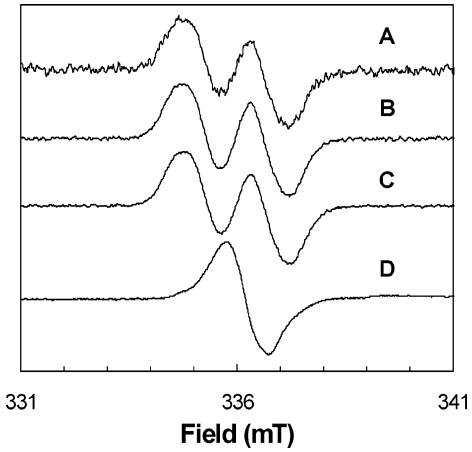

FIGURE 3: EPR spectra of the glycyl radical after in vitro activation. The EPR signals of partially purified native (14 U/mL, A) and recombinant Hpd (B) from *C. difficile* and Csd (C) from *C. scatologenes* are shown. Note that the 'residual' hydrogen at the glycyl radical site exchanges upon activation of Csd in D_2O (D). The spectra were recorded at 60 K (C), 77 K (A and D), or 100 K (B) at microwave power of 13 μW (A−C) or 50 μW (D). The microwave frequencies were 9.433−9.458 GHz using a modulation frequency of 100 kHz and modulation amplitude of 0.4 mT.

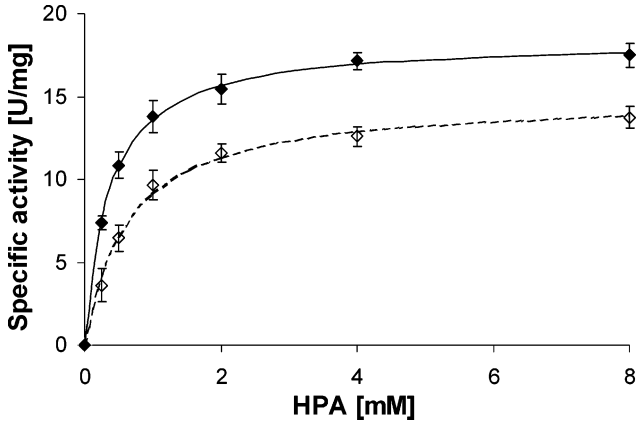

FIGURE 4: Michaelis−Menten kinetics of Csd (solid line) and Hpd (dashed line). The recombinant decarboxylases were activated with a 4-fold molar excess of recombinant AE (5 min at 30 °C). Then, aliquots of these samples were assayed in buffer containing the indicated substrate concentrations. The error bars refer to the standard deviation of three individual experiments. The average data were fitted to yield the values given in Table 2.

served for the recombinant enzymes never exceeded the limiting stoichiometry of one radical per hetero-octameric complex (0.8−1 spins/($\beta_4\gamma_4$)). The Hpd- and Csd-AEs were able to activate both decarboxylases.

C. scatologenes has been reported to produce *p*-cresol and 3-methylindole (scatole) from tyrosine and tryptophane, respectively (*21*). Csd turned out to be a genuine HPA decarboxylase. Hpd and Csd readily utilized HPA and 3,4-dihydroxyphenylacetate (DHPA), yielding the products *p*-cresol and 4-methylcatechol, respectively (Figure 4, Table 2). Neither phenylacetate, indole-3-acetate, nor 4-aminophenylacetate was decarboxylated.

The glycyl radical in Pfl was stable under anoxic conditions for several hours (*12*). In HPA decarboxylases, however, the radical decayed with a half-life of about 40 min in the absence of substrate (Figure 5). In the presence of substrate, however, no significant decrease of specific activity was observed, and cresol concentrations exceeding

Table 2: Kinetic Parameters of 4-Hydroxyphenylacetate Decarboxylases from *C. difficile* (Hpd) and *C. scatologenes* (Csd) with HPA or DHPA

enzyme	substrate	K_m (μM)	V_{max} (U/mg)	k_{cat} (s^{-1})	specificity constant (k_{cat}/K_m) ($mM^{-1}\,s^{-1}$)
Hpd	HPA	649 ± 90	14.97 ± 0.22	110	170
	DHPA	410 ± 52	8.82 ± 0.34	65	159
Csd	HPA	358 ± 20	18.45 ± 0.48	135	377
	DHPA	388 ± 28	9.12 ± 0.43	67	173

4 mM were attained (Figure 6). The rapid turnover by the activated decarboxylases and the comparable high protein concentrations needed in EPR sample disabled monitoring of the glycyl radical in the presence of substrate for extended time periods. Since the radical-free decarboxylase precursors were entirely inactive, it seems, however, reasonable to conclude that no significant radical dissipation takes place in the presence of HPA.

It has been previously shown that the native Hpd from *C. difficile* could be purified as a metal-free dimer of glycyl radical subunits (β_2), which was essentially inactive (*24*). Recombinant Hpd and Csd retained hetero-octameric quarternary structure after in vitro activation. The differences in the oligomeric states of recombinant and native enzymes were previously attributed to a reversible phosphorylation, which affected stability of the native complex (*23*). The glycyl radical subunit of recombinant Hpd was readily detectable with monoclonal antibodies against phosphoserine (Figure 7), indicating phosphorylation of a serinyl residue in the recombinant enzyme. Monoclonal antibodies against phosphotyrosine and phosphothreonine did not react with recombinant Hpd. Notably, the serine phosphorylation of Hpd was also detected in freshly prepared extracts from *C. difficile* cells grown in medium containing HPA, which causes specific induction of the enzyme (Figure 7). Notably, the serine phosphorylation of native Hpd was very unstable in extracts, and an incubation for only 10 min at 30 °C completely abolished phosphoserine detection and enzyme activity (*24*). The detection of serine phosphorylation in the glycyl radical subunits of Hpd, but also in Csd (not shown), suggests that control of activity via reversible phosphorylation might be a general feature of HPA decarboxylases.

DISCUSSION

HPA decarboxylases evidently form a distinct subclass within the emerging family of GREs. This subclass of GREs is characterized by the presence of small subunits, which are essential for enzymatic activity (*4*). HPA decarboxylases and Bss are the only iron−sulfur proteins among GREs. No obvious motifs for binding of iron−sulfur centers are present in the glycyl radical subunits of these enzymes. Interestingly, Bss contains two small subunits (*19*, *28*), which are not phylogenetically related to the small decarboxylase subunits. Since catalytically almost inactive, homodimeric Hpd has been purified as a metal-free protein from *C. difficile* (*24*), it is likely that the ligands for the iron−sulfur centers in HPA decarboxylases are provided by the small subunits. The amino acid sequence identity between the small subunits of Hpd and Csd is 41%, and four cysteinyl residues in the C-terminal part of the polypeptides are strictly conserved.

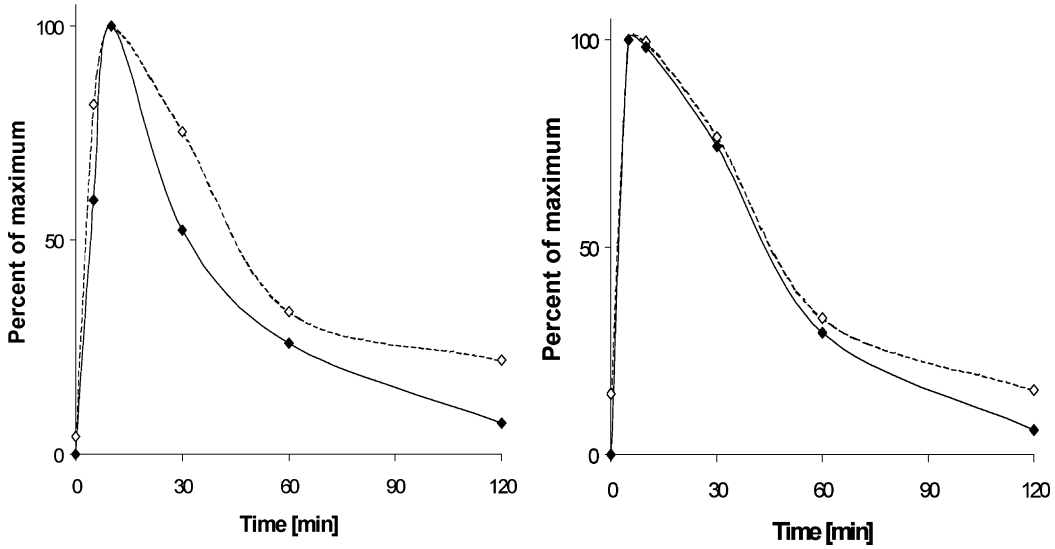

FIGURE 5: Transient activation of Hpd (left) and Csd (right) without substrate. Samples were prepared with different incubation times after addition of SAM and measured as in Figure 2D. Normalized values are shown for EPR intensities (100% = 9 ± 1 μM glycyl radical, closed diamonds) and specific activities (100% = 11 ± 2 U/mg, open diamonds).

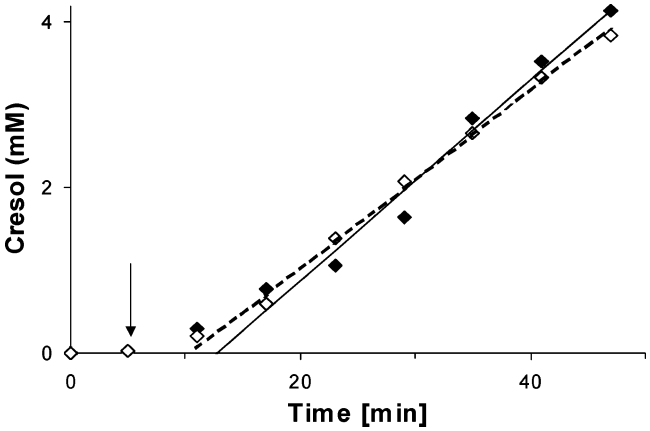

FIGURE 6: Activation of HPA decarboxylases in the presence of HPA (25 mM). The samples (10 μg/mL decarboxylases and 13.5 μg/mL AE) were prereduced with sodium dithionite (1 mM) in assay buffer prior to addition of SAM (arrow). At the time points indicated, samples were withdrawn and analyzed for *p*-cresol formation. Closed diamonds and solid line, Hpd; open diamonds and dashed line, Csd. Both enzymes exhibited similar specific activities (12 ± 2 U/mg) after about 10 min of activation.

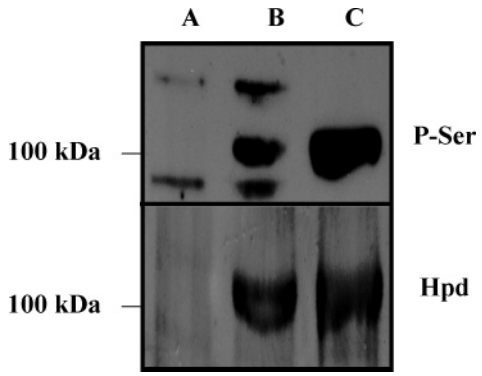

FIGURE 7: Serine phosphorylation of the glycyl radical subunit of Hpd. Cell-free extracts (25 μg total protein) of *C. difficile* grown overnight in a defined minimal medium with (B) or without (A) HPA were separated by SDS−PAGE. Proteins were transferred onto nitrocellulose membranes, and phosphoserine (upper panel) was detected with monoclonal antibodies. After the membranes were stripped with NaOH/SDS, Hpd was localized with polyclonal rabbit antiserum (lower panel). Recombinant Hpd (250 ng, C) was a positive control.

These putative metal ligands are located in a $Cx_2Cx_{13}Cx_{17}C$ motif, which is exclusively found in the small decarboxylase subunits. Despite low similarity between the amino acid sequences of the small subunits of Bss and GRE decarboxylases, the small Bss subunits may bind metal centers, because four cysteines with similar spacing are found in each of these proteins ($Cx_2C_{12-19}Cx_{22}C$) (*19*, *20*, *29*, *30*). The N-terminal part of small decarboxylase subunits may provide ligands for binding of a second iron−sulfur cluster. This center is less certain and likely contains three sulfur and one nitrogen ligand ($Hx_2Cx_{3-7}Cx_{4-5}C$). Nevertheless, its presence is suggested by the metal content of Hpd and Csd (32Fe/$\beta_4\gamma_4$), which accounts for eight [4Fe−4S] clusters in the hetero-octameric stucture.

The spin integration of glycyl radical (1/$\beta_4\gamma_4$) and reduced [4Fe−4S] centers (1−3/$\beta_4\gamma_4$) suggests that both paramagnetic centers are present in individual octamers. Accepting this view, we find that the lack of paramagnetic coupling between the glycyl radical and the metal centers suggests a distance >15 Å. This notion is further supported by structural considerations. Despite low amino acid sequence similarity, all known GRE structures exhibit a very similar fold (*15*, *16*, *18*, *24*, *31*), and the accommodation of an additional polypeptide in the vicinity of the active site is very unlikely.

Whereas the glycyl radical persists anaerobically for several hours in Pfl (*12*), it is comparably short-lived in HPA decarboxylases. Initial rapid accumulation of the radical, followed by a slow decline in its intensity correlated with loss of enzyme activity, suggests that radical quenching is significantly slower than radical formation. The continued dissipation of the radical after removal of the AE by gel filtration (data not shown) implies that the limited stability of the glycyl radical is an intrinsic property of the decarboxylases. The transfer of a second electron from the unique [4Fe−4S] clusters to the glycyl radical, followed by the protonation of the carbanion thus formed, could provide a mechanism for radical dissipation. Although the reduction of the radical by iron−sulfur centers is chemically unfavorable, the protonation of the carbanion might pull the

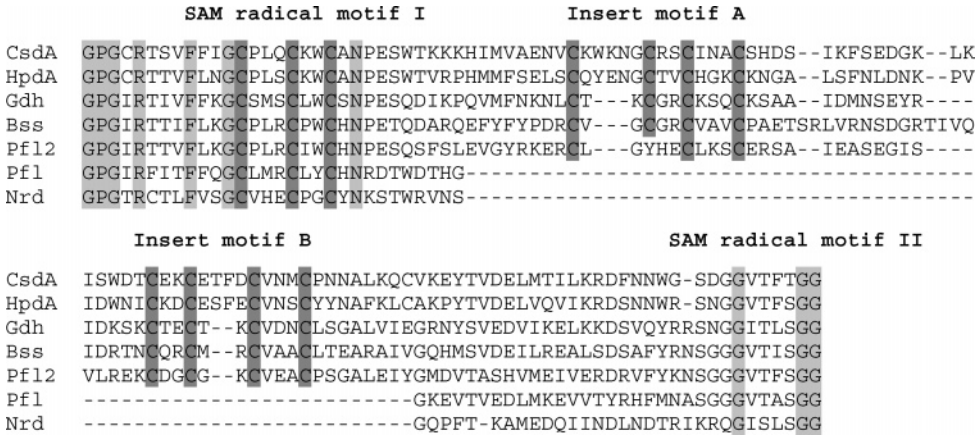

FIGURE 8: Partial sequence alignment of GRE-AEs. The sequences from the SAM cluster motif I to motif II for Csd- (*C. scatologenes*), Hpd- (*C. difficile*), Gdh- (*Clostridium butyricum*), Bss- (*T. aromatica*), Pfl2- (*A. fulgidus*), Pfl- (*E. coli*), and Nrd-AE (*E. coli*) are shown. Conserved residues are shaded light gray, putative metal ligands dark gray.

equilibrium toward the elimination of the radical. A similar reaction has been suggested for inactivation of methylmalonyl-CoA mutase by its suicide substrate allylmalonyl-CoA, where Co^{2+} reduces a substrate-derived allylic radical (*32*). This proposal is in line with the previously studied radical quenching in Pfl, which has been shown to be mediated by the multimeric alcohol dehydrogenase AdhE in *E. coli* (*33*, *34*). Sodium dithionite, however, has been shown to reduce the metal centers in the decarboxylases and the AEs at the same time. The individual processes might be dependent on different electron sources in living cells. This could avoid futile cycles and might allow independent regulation of both processes in vivo.

Transient radical formation in the absences of substrate is accompanied by an almost complete conversion of SAM to 5′-deoxyadenosine. Activation of decarboxylases and radical dissipation might therefore occur simultaneously under these conditions, and the observed net inactivation might be a result of SAM limitation. Notably, in the presence of substrate, only 1 equiv of 5′-desoxyadenosine per decarboxylase octamer is rapidly formed, suggesting that the radical dissipation is slower or might completely stop in the presence of substrate (Blaser, M., unpublished work).

The oligomeric state of the GRE decarboxylases distinguishes these enzymes from other GREs. The previously studied Pfl (*17*), Nrd (*15*), and Gdh (*18*) are homodimers of glycyl radical subunits, while Bss forms heterohexamers ($\alpha_2\beta_2\gamma_2$) (*19*). Only very recently, the crystal structure of the Pfl2 from *Archaeoglobus fulgidus* has been solved, suggesting that this enzyme forms a homotetramer (*31*). However, with regard to the glycyl radical subunits, all these enzymes are functional dimers, which carry one radical per dimer, and the dimerization of two of these dimers in Pfl2 has been suggested to provide structural adaptation to hyperthermophilic growth of *A. fulgidus*. In contrast, HPA decarboxylases apparently form functional octamers, which are essential for activation and contain only one radical in the catalytically active complex. The view that the hetero-octameric decarboxylases are the activation-competent and catalytically active state is supported by the observation that enzyme inactivation accompanied the loss of small subunits (*23*, *24*). Moreover, coexpression experiments of the glycyl radical subunit gene *hpdB* with the small subunit gene *csdC* yielded soluble, heterotetrameric hybrid decarboxylase, which could not be activated to the radical form by the available AEs (Yu, L., unpublished work).

Complex decay and concomitant activity loss were observed for the endogenous Hpd from *C. difficile* at elevated temperatures (*24*). The serine phosphorylation of the glycyl radical subunit suggests that phosphorylation-dependent regulation might be of physiological relevance. According to our hypothetical model, the small subunits recognize serine phosphorylation of the glycyl radical subunit, thereby inducing hetero-octamer assembly, which is the activation-competent and catalytically active state of the enzyme. If this hypothesis is correct, the dephosphorylation may cause complex decay and enzyme inactivation. Interestingly, the phosphorylation of the glycyl radical subunit precursors is also carried out in *E. coli*, while the dephosphorylation only occurs in *C. difficile*, suggesting that a specific phosphatase reaction is involved.

Decarboxylase AEs evidently contain one or two iron−sulfur center(s), which are most likely coordinated by a 60 amino acid insert between the SAM cluster motif (GCx_3Cx_2CxN) and the SAM-binding motif II (Gx_4GG) (*5*). The insert provides eight cysteinyl ligands for up to two [4Fe−4S] centers, which show an unusual spacing of the cysteines, that is, $Cx_5Cx_2Cx_3C$ and $Cx_2Cx_4Cx_3C$. Interestingly, similar inserts (providing one or both motifs) are found in all GRE-AEs with the exception of Pfl- and Nrd-AEs (*4*) (Figure 8), suggesting that these AEs also contain additional iron−sulfur clusters.

There is striking spectroscopic evidence that SAM binds directly to an unique [4Fe−4S] cluster close to the N-terminus of the GRE-AEs (*35*, *36*). The crystal structures of related members of the SAM radical enzyme superfamily, including HemN (*37*) and lysine-2,3-aminomutase (*38*), show that SAM is coordinated via its methionine moiety to the free iron site of this [4Fe−4S] center. The tight binding causes distinct changes in the EPR spectra of Pfl- (*39*) and Nrd-AE (*9*) upon addition of SAM. Although a similar binding mode can be predicted for the decarboxylase AEs, no significant SAM-dependent changes of the EPR signals of the reduced [4Fe−4S] centers were found. Hence, it is likely that the insert cluster(s) were preferentially reduced under the experimental conditions. If this assumption is correct, an efficient reduction of the SAM cluster in decarboxylase AEs might occur only upon binding of the

decarboxylases, that is, in the Michaelis−Menten complex of the activation process. The view that additional iron−sulfur clusters might be involved in electron transfer to SAM has been very recently supported by mutagenesis studies affecting the putative cysteine ligands provided by the insert motifs. All mutations affecting the SAM cluster yielded inactive AEs and abolished homolytic cleavage of SAM. Insert cluster mutants slowed radical formation and generated 5′-deoxyadenosine about 50- to 100-fold slower than wild-type AE (Blaser, M., unpublished work).

In conclusion, HPA decarboxylases clearly differ structurally and functionally from previously studied Pfl and Nrd systems. Metal content and oligomeric state of the enzymes appear to be controlled by small subunits, which are essential constituents of the enzymes and offer unique regulatory properties to HPA decarboxylases. While intrinsic radical dissipation may provide a reversible 'switch-off' mechanism in the absence of substrate, the phosphorylation-dependent control of activity via the oligomeric state may allow regulation of cresol formation beyond the intermediate catalytic process in response to external triggers. It is likely that such triggers may arise from the various metabolic situations the bacteria must face in highly competitive environments such as the mammalian large intestine.

ACKNOWLEDGMENT

We thank Silke Werner and Marc Friedrich, for technical assistance, and Wolfgang Buckel, Dan Darley, and Gary Sawers for critically reading of the manuscript.

REFERENCES

1. Eklund, H., and Fontecave, M. (1999) Glycyl radical enzymes: a conservative structural basis for radicals, *Struc. Folding Des. 7*, R257−262.
2. Fontecave, M. (1998) Ribonucleotide reductases and radical reactions, *Cell. Mol. Life Sci. 54*, 684−695.
3. Sawers, G., and Watson, G. (1998) A glycyl radical solution: oxygen-dependent interconversion of pyruvate formate-lyase, *Mol. Microbiol. 29*, 945−954.
4. Selmer, T., Pierik, A. J., and Heider, J. (2005) New glycyl radical enzymes catalysing key metabolic steps in anaerobic bacteria, *Biol. Chem. 386*, 981−988.
5. Sofia, H. J., Chen, G., Hetzler, B. G., Reyes-Spindola, J. F., and Miller, N. E. (2001) Radical SAM, a novel protein superfamily linking unresolved steps in familiar biosynthetic pathways with radical mechanisms: functional characterization using new analysis and information visualization methods, *Nucleic Acids Res. 29*, 1097−1106.
6. Tamarit, J., Gerez, C., Meier, C., Mulliez, E., Trautwein, A., and Fontecave, M. (2000) The activating component of the anaerobic ribonucleotide reductase from *Escherichia coli*. An iron−sulfur center with only three cysteines, *J. Biol. Chem. 275*, 15669−15675.
7. Tamarit, J., Mulliez, E., Meier, C., Trautwein, A., and Fontecave, M. (1999) The anaerobic ribonucleotide reductase from *Escherichia coli*. The small protein is an activating enzyme containing a $[4Fe\text{-}4S]^{2+}$ center, *J. Biol. Chem. 274*, 31291−31296.
8. Ollagnier, S., Mulliez, E., Gaillard, J., Eliasson, R., Fontecave, M., and Reichard, P. (1996) The anaerobic *Escherichia coli* ribonucleotide reductase. Subunit structure and iron sulfur center, *J. Biol. Chem. 271*, 9410−9416.
9. Ollagnier, S., Mulliez, E., Schmidt, P. P., Eliasson, R., Gaillard, J., Deronzier, C., Bergman, T., Graslund, A., Reichard, P., and Fontecave, M. (1997) Activation of the anaerobic ribonucleotide reductase from *Escherichia coli*. The essential role of the iron−sulfur center for S-adenosylmethionine reduction, *J. Biol. Chem. 272*, 24216−24223.
10. Kuelzer, R., Pils, T., Kappl, R., Huttermann, J., and Knappe, J. (1998) Reconstitution and characterization of the polynuclear iron−sulfur cluster in pyruvate formate-lyase-activating enzyme. Molecular properties of the holoenzyme form, *J. Biol. Chem. 273*, 4897−4903.
11. Sun, X., Eliasson, R., Pontis, E., Andersson, J., Buist, G., Sjoberg, B. M., and Reichard, P. (1995) Generation of the glycyl radical of the anaerobic *Escherichia coli* ribonucleotide reductase requires a specific activating enzyme, *J. Biol. Chem. 270*, 2443−2446.
12. Walsby, C. J., Ortillo, D., Yang, J., Nnyepi, M. R., Broderick, W. E., Hoffman, B. M., and Broderick, J. B. (2005) Spectroscopic approaches to elucidating novel iron−sulfur chemistry in the "radical-SAM" protein superfamily, *Inorg. Chem. 44*, 727−741.
13. Unkrig, V., Neugebauer, F. A., and Knappe, J. (1989) The free radical of pyruvate formate-lyase. Characterization by EPR spectroscopy and involvement in catalysis as studied with the substrate-analogue hypophosphite, *Eur. J. Biochem. 184*, 723−728.
14. Wagner, A. F., Frey, M., Neugebauer, F. A., Schäfer, W., and Knappe, J. (1992) The free radical in pyruvate formate-lyase is located on glycine-734, *Proc. Natl. Acad. Sci. U.S.A. 89*, 996−1000.
15. Logan, D. T., Andersson, J., Sjoberg, B. M., and Nordlund, P. (1999) A glycyl radical site in the crystal structure of a class III ribonucleotide reductase, *Science 283*, 1499−1504.
16. Becker, A., and Kabsch, W. (2002) X-ray structure of pyruvate formate-lyase in complex with pyruvate and CoA. How the enzyme uses the Cys-418 thiyl radical for pyruvate cleavage, *J. Biol. Chem. 277*, 40036−40042.
17. Becker, A., Fritz-Wolf, K., Kabsch, W., Knappe, J., Schultz, S., and Volker Wagner, A. F. (1999) Structure and mechanism of the glycyl radical enzyme pyruvate formate-lyase, *Nat. Struct. Biol. 6*, 969−975.
18. O'Brien, J. R., Raynaud, C., Croux, C., Girbal, L., Soucaille, P., and Lanzilotta, W. N. (2004) Insight into the mechanism of the B_{12}-independent glycerol dehydratase from *Clostridium butyricum*: preliminary biochemical and structural characterization, *Biochemistry 43*, 4635−4645.
19. Leuthner, B., Leutwein, C., Schulz, H., Horth, P., Haehnel, W., Schiltz, E., Schagger, H., and Heider, J. (1998) Biochemical and genetic characterization of benzylsuccinate synthase from *Thauera aromatica*: a new glycyl radical enzyme catalysing the first step in anaerobic toluene metabolism, *Mol. Microbiol. 28*, 615−628.
20. Coschigano, P. W., Wehrman, T. S., and Young, L. Y. (1998) Identification and analysis of genes involved in anaerobic toluene metabolism by strain T1: putative role of a glycine free radical, *Appl. Environ. Microbiol. 64*, 1650−1606.
21. Elsden, S. R., Hilton, M. G., and Waller, J. M. (1976) The end products of the metabolism of aromatic amino acids by Clostridia, *Arch. Microbiol. 107*, 283−288.
22. D'Ari, L., and Barker, H. A. (1985) *p*-Cresol formation by cell-free extracts of *Clostridium difficile*, *Arch. Microbiol. 143*, 311−312.
23. Andrei, P. I., Pierik, A. J., Zauner, S., Andrei-Selmer, L. C., and Selmer, T. (2004) Subunit composition of the glycyl radical enzyme *p*-hydroxyphenylacetate decarboxylase. A small subunit, HpdC, is essential for catalytic activity, *Eur. J. Biochem. 271*, 2225−2230.
24. Selmer, T., and Andrei, P. I. (2001) *p*-Hydroxyphenylacetate decarboxylase from *Clostridium difficile*. A novel glycyl radical enzyme catalysing the formation of *p*-cresol, *Eur. J. Biochem. 268*, 1363−1372.
25. Pierik, A. J., Wolbert, R. B., Mutsaers, P. H., Hagen, W. R., and Veeger, C. (1992) Purification and biochemical characterization of a putative [6Fe-6S] prismane-cluster-containing protein from *Desulfovibrio vulgaris* (Hildenborough), *Eur. J. Biochem. 206*, 697−704.
26. Karasawa, T., Ikoma, S., Yamakawa, K., and Nakamura, S. (1995) A defined growth medium for *Clostridium difficile*, *Microbiology 141* (Pt 2), 371−375.
27. Verfürth, K., Pierik, A. J., Leutwein, C., Zorn, S., and Heider, J. (2004) Substrate specificities and electron paramagnetic resonance properties of benzylsuccinate synthases in anaerobic toluene and *m*-xylene metabolism, *Arch. Microbiol. 181*, 155−162.
28. Leuthner, B., and Heider, J. (2000) Anaerobic toluene catabolism of *Thauera aromatica*: the bbs operon codes for enzymes of beta oxidation of the intermediate benzylsuccinate, *J. Bacteriol. 182*, 272−277.
29. Rabus, R., Kube, M., Heider, J., Beck, A., Heitmann, K., Widdel, F., and Reinhardt, R. (2005) The genome sequence of an anaerobic

aromatic-degrading denitrifying bacterium, strain EbN1, *Arch. Microbiol. 183*, 27−36.
30. Kube, M., Heider, J., Amann, J., Hufnagel, P., Kuhner, S., Beck, A., Reinhardt, R., and Rabus, R. (2004) Genes involved in the anaerobic degradation of toluene in a denitrifying bacterium, strain EbN1, *Arch. Microbiol. 181*, 182−194.
31. Lethiö, L., Grossmann, J., Kokona, B., Fairman, R., and Goldman, A. (2006) Crystal structure of a glycyl radical enzyme from *Archaeoglobus fulgidus*, *J. Mol. Biol. 357*, 221−235.
32. Pandovani, D., and Banerjee, R. (2006) Alternative pathways for radical dissipation in an active site mutant of B_{12}-dependent methylmalonyl-CoA mutase, *Biochemistry 45*, 2951−2959.
33. Kessler, D., Herth, W., and Knappe, J. (1992) Ultrastructure and pyruvate formate-lyase radical quenching property of the multienzymic AdhE protein of *Escherichia coli*, *J. Biol. Chem. 267*, 18073−18079.
34. Kessler, D., Leibrecht, I., and Knappe, J. (1991) Pyruvate-formate-lyase-deactivase and acetyl-CoA reductase activities of *Escherichia coli* reside on a polymeric protein particle encoded by adhE, *FEBS Lett. 281*, 59−63.
35. Krebs, C., Broderick, W. E., Henshaw, T. F., Broderick, J. B., and Huynh, B. H. (2002) Coordination of adenosylmethionine to a unique iron site of the [4Fe-4S] of pyruvate formate-lyase: a Mössbauer spectroscopic study, *J. Am. Chem. Soc. 124*, 912−913.
36. Walsby, C. J., Ortillo, D., Broderick, W. E., Broderick, J. B., and Hoffman, B. M. (2002) An anchoring role for FeS clusters: chelation of the amino acid moiety of S-adenosylmethionine to the unique iron site of the [4Fe-4S] cluster of pyruvate formate-lyase activating enzyme, *J. Am. Chem. Soc. 124*, 11270−11271.
37. Layer, G., Moser, J., Heinz, D. W., Jahn, D., and Schubert, W. D. (2003) Crystal structure of coproporphyrinogen III oxidase reveals cofactor geometry of radical SAM enzymes *EMBO J. 22*, 6214−6224.
38. Lepore, B. W., Ruzicka, F. J., Frey, P. A., and Ringe, D. (2005) The X-ray crystal structure of lysine-2,3-aminomutase from *Clostridium subterminale*, *Proc. Natl. Acad. Sci. U.S.A. 102*, 13819−13824.
39. Walsby, C. J., Hong, W., Broderick, W. E., Cheek, J., Ortillo, D., Broderick, J. B., and Hoffman, B. M. (2002) Electron−nuclear double resonance spectroscopic evidence that *S*-adenosylmethionine binds in contact with the catalytically active $[4Fe-4S]^+$ cluster of pyruvate formate-lyase activating enzyme, *J. Am. Chem. Soc. 124*, 3143−3151.

BI060840B